

Towards Robust Offline-to-Online Reinforcement Learning via Uncertainty and Smoothness

Xiaoyu Wen^{1*}, Xudong Yu^{2*}, Rui Yang³, Chenjia Bai^{4,5†} Zhen Wang^{1†}

¹Northwestern Polytechnical University, ²Harbin Institute of Technology, ³HKUST,

⁴Shanghai Artificial Intelligence Laboratory, ⁵Shenzhen Research Institute of Northwestern Polytechnical University
wenxiaoyu@mail.nwpu.edu.cn, hit20byu@gmail.com, ryangam@connect.ust.hk, baichenjia@pjlab.org.cn,
w-zhen@nwpu.edu.cn

Abstract

To obtain a near-optimal policy with fewer interactions in Reinforcement Learning (RL), a promising approach involves the combination of offline RL, which enhances sample efficiency by leveraging offline datasets, and online RL, which explores informative transitions by interacting with the environment. Offline-to-Online (O2O) RL provides a paradigm for improving an offline trained agent within limited online interactions. However, due to the significant distribution shift between online experiences and offline data, most offline RL algorithms suffer from performance drops and fail to achieve stable policy improvement in O2O adaptation. To address this problem, we propose the Robust Offline-to-Online (RO2O) algorithm, designed to enhance offline policies through uncertainty and smoothness, and to mitigate the performance drop in online adaptation. Specifically, RO2O incorporates Q-ensemble for uncertainty penalty and adversarial samples for policy and value smoothness, which enable RO2O to maintain a consistent learning procedure in online adaptation without requiring special changes to the learning objective. Theoretical analyses in linear MDPs demonstrate that the uncertainty and smoothness lead to a tighter optimality bound in O2O against distribution shift. Experimental results illustrate the superiority of RO2O in facilitating stable offline-to-online learning and achieving significant improvement with limited online interactions.

Introduction

Reinforcement learning (RL) has demonstrated remarkable success in tackling complex tasks, such as playing games (Lample and Chaplot 2017; Hessel et al. 2018; Silver et al. 2018; Aytar et al. 2018) and controlling robots (Schulman et al. 2015, 2017; Haarnoja et al. 2018) in recent years. Nonetheless, persistent critiques point to its limited adaptability in real-world scenarios. The efficacy of RL critically hinges upon access to an unbiased interactive environment and the luxury of conducting millions of unrestricted trial-and-error attempts (Mnih et al. 2015; Wang et al. 2016). However, domains such as healthcare (Miotto et al. 2018) and autonomous driving (Bojarski et al. 2016; Kiran et al. 2021) often present challenges in data collection due to safety, feasibility, and financial reasons.

Offline RL presents a distinctive advantage over online RL, as it enables the learning of policies directly from a fixed

dataset collected by a behavior policy (Levine et al. 2020; Prudencio, Maximo, and Colombini 2023). These datasets can be sourced from historical logs, demonstrations, or expert knowledge, furnishing valuable information to facilitate learning without the need for costly online data collection. Nonetheless, the efficacy of current offline RL methods heavily relies on the coverage of the state-action space and the quality of stored trajectories (Schweighofer et al. 2022). Furthermore, the lack of exploration hampers the agent's ability to discover superior policies (Lambert et al. 2022). To address this issue, numerous studies focus on enhancing pre-trained offline agents through limited online interactions, known as Offline-to-Online (O2O) RL (Nair et al. 2020; Lee et al. 2022; Zhang, Xu, and Yu 2023). This paradigm aims to rectify estimation bias, which remains unaddressed during offline training, and lead to further policy improvement through several online fine-tuning steps.

Despite the potential to integrate offline datasets and online experiences to optimize the agent, existing offline-to-online learning methods suffer from performance drops and struggle to efficiently improve policies, which hinders their applicability in real-world scenarios. At the initial stage of online fine-tuning, the agent's performance may heavily decline due to the distributional shift between offline datasets and online transitions (Nair et al. 2020; Uchendu et al. 2023). Moreover, the inclusion of low-quality data can have detrimental effects on the performance and lead to skewed optimization. Prior efforts to address this issue involve altering the policy extraction procedure (Nair et al. 2020; Kostrikov, Nair, and Levine 2022), incorporating behavior cloning (BC) regularization (Zhao et al. 2022), modifying data sampling methods (Lee et al. 2022), or proposing policy expansion sets (Zhang, Xu, and Yu 2023). While these methods have made progress in mitigating performance drops, they often entail complex and task-specific implementations, such as adjusting the weights of BC regularization and the ratio of sampling from different data distributions. Furthermore, these approaches lack effective mechanisms to enhance performance during the fine-tuning phase.

In this paper, we propose the Robust Offline-to-Online (RO2O) algorithm for RL, designed to address the distribution shift in the O2O process and achieve efficient policy improvement during the fine-tuning stage. To achieve this, RO2O utilizes Q -ensembles to learn robust value functions,

*Equal Contribution †Corresponding Author

resulting in no performance drop during the initial stage of online fine-tuning. Notably, RO2O offers the advantage of not requiring the transformation of the learning algorithm (Zhao et al. 2023) or policy composition (Zhang, Xu, and Yu 2023) throughout the process. Additionally, RO2O incorporates robustness regularization by considering the resilience of policies and value functions to variations in observations. Specifically, the smoothness of policies and value functions on out-of-distribution states and actions is regularized, ensuring robust performance even when the interacting trajectories in the training buffer deviate significantly from offline policies. From a theoretical perspective, we prove that under the linear MDP assumption, the uncertainty and smoothness lead to a tighter optimality bound in O2O against distribution shift. Empirical results showcase the favorable performance of RO2O during both offline pre-training and online fine-tuning. Compared to baseline algorithms, RO2O achieves efficient policy improvement without the need for specific explorations or modifications to the learning architecture.

Related Work

Offline-to-Online RL A key challenge in O2O process is the performance drop experienced at the initial stage, attributed to the distributional shift between offline data and online experiences. Previous approaches have attempted to address this issue by altering policy extraction (Nair et al. 2020; Kostrikov, Nair, and Levine 2022), adjusting sampling methods (Lee et al. 2022), expanding policy sets (Zhang, Xu, and Yu 2023), and modifying Q -function learning targets (Nakamoto et al. 2023). However, these methods cannot consistently achieve effective policy improvement within the limited fine-tuning steps. Recently, ensembles have been incorporated for both pessimistic learning during offline training and optimistic exploration during online learning (Zhao et al. 2023). While such an ensemble method improves the O2O performance, it requires careful modifications of learning objectives when transferring the policy from offline to online stages. In contrast, our work handles offline training and online fine-tuning in a consistent manner without algorithmic modifications. The proposed approach not only achieves better offline performance but also enables efficient policy improvement during online fine-tuning.

Ensembles in RL Ensemble methods have emerged as a prominent and versatile approach in RL to enhance the value function for sample-efficient learning. In online RL, ensembles are utilized to capture epistemic uncertainty and improve exploration (Osband et al. 2016; Chen et al. 2017). Recent methods also employ ensembles to mitigate estimation bias during Bellman updates (Fujimoto, Hoof, and Meger 2018; Lan et al. 2020) or enhance sample efficiency (Chen et al. 2021). In the context of offline RL, ensembles are employed in both model-free methods (Bai et al. 2022; An et al. 2021a) and model-based methods (Yu et al. 2020) to characterize the uncertainty of Q -values or dynamics models. Notably, several works (An et al. 2021a; Ghasemipour, Gu, and Nachum 2022) estimate lower confidence bounds of Q -functions using ensembles, leading to state-of-the-art perfor-

mance in offline RL. Our method also utilizes Q -ensembles and presents its effectiveness to handle the distributional shift and to obtain policy improvement during fine-tuning.

Robustness in RL Robustness has gained paramount importance in RL to ensure the reliability and stability of RL agents in diverse and challenging environments. In online RL, previous research has explored techniques such as domain randomization (Tobin et al. 2017), policy smoothing (Shen et al. 2020), and data augmentation methods (Sinha, Mandlekar, and Garg 2022) to improve performance. Recently, an offline RL algorithm (Yang et al. 2022) incorporates policy and value smoothing for out-of-distribution (OOD) states, highlighting the significance of robustness in offline RL agents. These approaches typically focus on enhancing robustness against adversarial perturbations on observations or actions and validate their effectiveness through the synthesis of noisy data. In contrast, our focus is on the robustness of models to handle the distributional shift specifically in the offline-to-online RL setting.

Preliminaries

The RL problem is typically formulated as Markov Decision Process (MDP), represented by the tuple $\mathcal{M} = \{\mathcal{S}, \mathcal{A}, P, R, \gamma\}$. In this framework, the agent’s decision-making process is guided by a policy denoted as π , which maps environmental states, $s \in \mathcal{S}$ to actions $a \in \mathcal{A}$. The agent’s objective is to find an optimal policy, denoted as π^* , that maximizes the expected cumulative reward over time. For a policy π , the state-value function, denoted as $Q^\pi(s, a)$, represents the expected cumulative reward starting from state s , taking action a , and following policy π thereafter. The learning target for the value function in online RL, also referred to as the Bellman operator, can be expressed as:

$$\mathcal{T}Q(s, a) = r(s, a) + \gamma \mathbb{E}_{s' \sim P(\cdot|s, a), a' \in \pi(\cdot|s)} Q(s', a'). \quad (1)$$

In offline RL, learning is performed using a fixed dataset $\mathcal{D} = \{s_i, a_i, r_i, s'_i\}_{i=1}^n$ of historical interactions sampled from a behavior policy μ . A key challenge in offline RL is the bootstrapped error caused by the distributional shift between behavior policies and learned policies. To mitigate the distributional shift, previous methods (Bai et al. 2022; Yang et al. 2022) leverage Q -ensembles to capture epistemic uncertainty and penalize Q -functions with large uncertainties. The Bellman operator becomes $\widehat{\mathcal{T}}Q(s, a) = r(s, a) + \gamma \widehat{\mathbb{E}}_{s' \sim P(\cdot|s, a), a' \sim \pi(\cdot|s')} (Q(s', a') - \alpha U(s', a'))$, where we estimate the empirical expectation from the dataset \mathcal{D} , $U(s', a')$ denotes the estimated uncertainties, and α adjusts the degree of pessimism. Additionally, RORL (Yang et al. 2022) employs smooth regularization on the policy and the value function for states near the dataset.

Despite the advantage of leveraging large-scale offline data, the performance of pre-trained agents is often limited by the optimality and coverage of the datasets. Overestimation of value functions cannot be substantially corrected without interactions with the environment. To address this limitation, our work focuses on O2O learning, aiming to improve agents by incorporating limited online interactions.

Methodology

In this section, we present our methodology for addressing the challenges posed by the offline-to-online RL setting. The most significant challenge in this context is effectively transferring knowledge from the static dataset to cope with distributional shift in the dynamic online environment. To tackle this crucial issue, we propose the RO2O algorithm, a novel approach that combines Q -ensembles and robustness regularization. We begin by providing a motivating example to illustrate that current methods struggle to handle a large distributional shift effectively. Subsequently, we introduce our algorithm, which maintains a consistent architecture in both offline and online learning phases. Furthermore, we establish theoretical support for our approach.

Motivating Example

Offline-to-Online RL methods face challenges arising from distribution shift not only between learned policies and behavior policies but also between offline data and online transitions during the fine-tuning process. Robust performance is expected from offline algorithms despite the presence of online trajectories that deviate from the learned offline policies. To investigate this, we evaluate two state-of-the-art offline methods, i.e., CQL and IQL, with distinct distribution shifts to simulate the O2O process. Specifically, we pre-train the agents using the halfcheetah-expert dataset from D4RL (Fu et al. 2020) benchmark, and inject synthetic distributional shift similar to that in online fine-tuning process to assess their robustness. The synthetic distributional shift is incorporated by adding samples from a different offline dataset, such as the halfcheetah-medium dataset. As depicted in the left panel of Figure 1, noticeable discrepancies in the trajectory distribution exist between the two datasets, indicating the presence of distributional shift.

We compare the performance of CQL, IQL, and our method to figure out whether the state-of-the-art methods can handle the synthetic distributional shift during fine-tuning. The experimental results are shown in the right panel of Figure 1. Our findings reveal that all methods experience a performance drop at the initial stage due to the significant distributional shift. However, in comparison to CQL and IQL, our method exhibits a milder degradation in performance. Moreover, CQL and IQL fail to recover from the deviation during the fine-tuning phase with a new dataset. This inability is attributed to the presence of samples that deviate significantly from the region covered by the current policies, which affects the learning of policies and value functions. In contrast, our method demonstrates superior robustness, enabling effective policy improvement even in the presence of significant distributional shifts. As previously mentioned, it is expected to correct estimation bias and improve pre-trained policies within limited online interactions, while traditional methods struggle to accomplish this.

Algorithm

Based on the motivating example, we suggest that it is important to design a robust algorithm capable of ensuring stable policy improvement with online interactions. To this end,

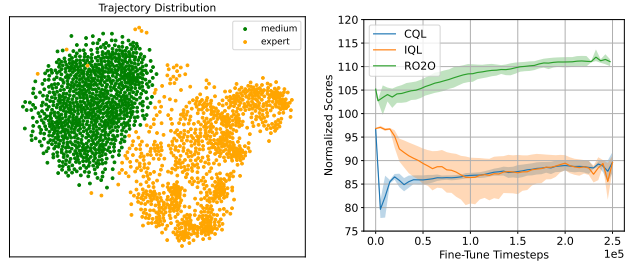


Figure 1: Illustration for the motivating example. In the left panel, we visualize the trajectory distribution of two datasets, by mapping the trajectories into two-dimensional points using T-SNE (Van der Maaten and Hinton 2008). The right panel presents the fine-tuning performance.

we propose the RO2O method, which incorporates ensembles and robustness regularization into the offline-to-online learning process. Notably, our method stands out from other existing approaches, such as PEX (Zhang, Xu, and Yu 2023) and E2O (Zhao et al. 2023), due to its unique characteristics. Unlike these methods, our approach does not require any changes to the learning algorithm or the need to conduct policy expansion when transitioning to the fine-tuning stage.

Ensemble-based Offline-to-Online Learning In our method, we adopt Q -ensemble with N networks in both offline pre-training and online fine-tuning, employing the same update procedure. These ensemble networks possess identical architecture and are initialized independently. While prior studies (Chen et al. 2021; Zhao et al. 2023) suggest that randomly selecting two of the N ensembles is effective during the online learning phase, our findings indicate that choosing the *minimum* of ensemble Q -functions is sufficient to achieve favorable performance. Moreover, this choice remains consistent with the offline learning process, where pessimism is necessary to counteract overestimation bias. Formally, the TD target when using the minimum of ensemble Q -functions can be expressed as:

$$\widehat{\mathcal{T}}Q_{\theta_i}(s, a) = r(s, a) + \gamma \widehat{\mathbb{E}}_{s'} \min_i Q_{\theta_i^-}(s', a'), i \in [1, N], \quad (2)$$

where θ_i and θ_i^- are parameters for i -th Q -network and target Q -network, respectively, and $a' \sim \pi(s')$. For the challenging AntMaze environments, we adhere to previous work (Ghasemipour, Gu, and Nachum 2022) and utilize *independent* Bellman targets without altering the network architecture. Similarly, independent targets can be formulated as:

$$\widehat{\mathcal{T}}Q_{\theta_i}(s, a) = r(s, a) + \gamma \widehat{\mathbb{E}}_{s'} Q_{\theta_i^-}(s', a'), i \in [1, N]. \quad (3)$$

During offline training, the Q -ensembles are utilized to learn the value function and update the policy. In online fine-tuning, the learned Q -ensembles and policies continue to be updated with online experiences, as shown in Figure 2. Several online RL methods (Chen et al. 2021; Lee et al. 2021) also employ Q -ensembles and suggest maximizing the average Q -values for policy optimization. In our study, we have found that maximizing the minimum Q -values, consistent

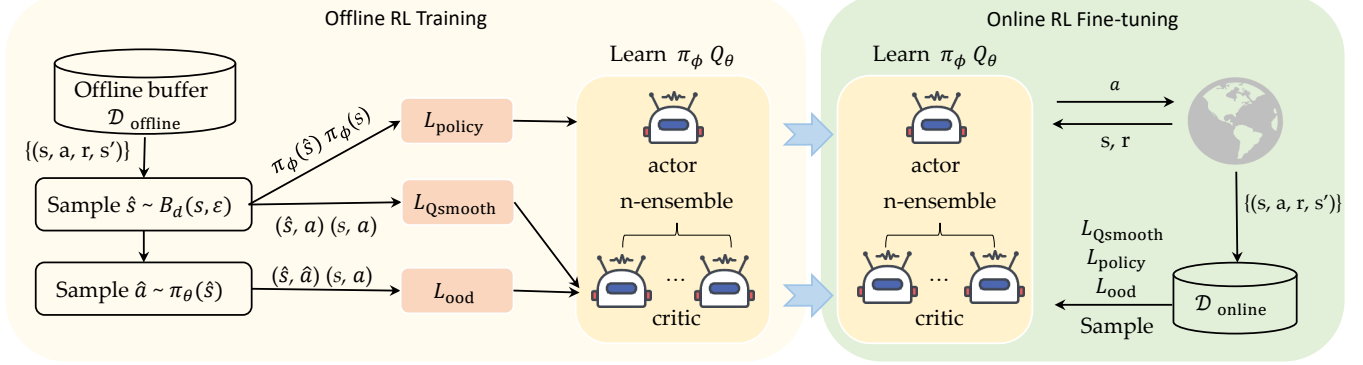


Figure 2: **Overall framework of RO2O.** RO2O employs the same off-policy RL algorithms during the offline-to-online training phase. By using OOD sampling, we incorporate \mathcal{L}_{ood} and $\mathcal{L}_{\text{Qsmooth}}$ into the training process for the gradient update, while also calculating $\mathcal{L}_{\text{policy}}$ to constrain the policy $\pi_\phi(\hat{s})$ as close as possible to the current policy $\pi_\phi(s)$.

with the objective in the offline stage, is also highly effective in obtaining the optimal policy during online fine-tuning.

Robustness Regularization Similar to previous studies (Sinha, Mandlekar, and Garg 2022; Shen et al. 2020) that consider robustness in RL, our aim is to enhance the robustness of offline-trained value function and policy, which can have large estimation bias caused by the distribution shift in the fine-tuning phase. Different from previous offline RL approaches that mainly mitigate the effect of perturbed actions (Zhao et al. 2022; Nakamoto et al. 2023), we adopt a different robustness perspective by suggesting that the distributional shift in O2O process brings both OOD states and actions. As a result, we enhance the robustness of value function and policy with OOD states and actions to ensure stable learning and improvement. Specifically, the Q -function and policy should be enforced not to generate large fluctuations for transitions nearby the offline dataset, which leads to smooth value function and policy that are robust to distribution shift. To this end, we follow a similar approach as in Yang et al. (2022) to construct adversarial samples for regularization in the O2O process.

We employ regularization on both policy and Q -function by minimizing the difference between estimations obtained from in-sample data and perturbed samples. Specifically, we synthesize perturbed samples by constructing a perturbation set $\mathbb{B}_d(s, \epsilon) = \{\hat{s} : d(s, \hat{s}) \leq \epsilon\}$ for state s , which is an ϵ -radius ball with a distance metric $d(\cdot, \cdot)$. By sampling from this set $\hat{s} \in \mathbb{B}_d(s, \epsilon)$, the proposed RO2O minimizes the difference between $Q_{\theta_i}(s, a)$ and $Q_{\theta_i}(\hat{s}, a)$, as

$$\mathcal{L}_{\text{Qsmooth}} = \mathcal{L}(Q_{\theta_i}(s, a), Q_{\theta_i}(\hat{s}, a)), \quad (4)$$

which enforces value smoothness to adversarial state \hat{s} , and \mathcal{L} can be a L_2 distance. The smooth loss should be applied to each network in the ensemble. To simplify the optimization, we choose to minimize the maximal smooth loss $\max_i \mathcal{L}_{\text{Qsmooth}}$ among the ensemble. Similarly, we can minimize the difference between $\pi(a|s)$ and $\pi(a|\hat{s})$, which is realized by minimizing the JS divergence $D_J(\pi(\cdot|s) \parallel \pi(\cdot|\hat{s}))$.

Meanwhile, since the Q -values for OOD states and actions can be overestimated, we penalize their value estimation with uncertainty quantification following prior works

(Bai et al. 2022; Yang et al. 2022). For OOD states $\hat{s} \in \mathbb{B}_d(s, \epsilon)$ and OOD actions $\hat{a} \sim \pi(\hat{s})$, their pseudo Bellman targets can be expressed as $\hat{\mathcal{T}}^{\text{ood}} Q(\hat{s}, \hat{a}) = Q(\hat{s}, \hat{a}) - \alpha U(\hat{s}, \hat{a})$. Let θ_i be the parameters of the i -th Q function, we have a loss function to constrain the value of OOD samples:

$$\mathcal{L}_{\text{ood}} = \mathbb{E}_{\hat{s} \in \mathbb{B}_d(s, \epsilon), \hat{a} \sim \pi(\hat{s})} (\hat{\mathcal{T}}^{\text{ood}} Q_{\theta_i}(\hat{s}, \hat{a}) - Q_{\theta_i}(\hat{s}, \hat{a}))^2. \quad (5)$$

Algorithm Description As outlined in Algorithm 1, the learning process encompasses two phases: offline pre-training and online fine-tuning. We adopt the SAC (Haarnoja et al. 2018) algorithm as our backbone. For Q -value functions, RO2O has the following loss function:

$$\mathcal{L}_Q = \mathbb{E}_{(s, a, r, s') \sim \mathcal{D}} [\mathcal{L}_{\text{TD}} + \eta_1 \mathcal{L}_{\text{Qsmooth}} + \eta_2 \mathcal{L}_{\text{ood}}], \quad (6)$$

where $\mathcal{D} = \mathcal{D}_{\text{offline}}$ in the offline training stage and $\mathcal{D} = \mathcal{D}_{\text{offline}} \cup \mathcal{D}_{\text{online}}$ in the online fine-tuning stage. $\mathcal{L}_{\text{TD}} = (\mathcal{T}Q_{\theta_i}(s, a) - Q_{\theta_i}(s, a))^2$ represents the TD error, where $\mathcal{T}Q_{\theta_i} = r + \gamma \left(\min_i Q_{\theta_i}(s', a') - \beta \log \pi(a'|s') \right)$ when taking shared targets in Equation 2 for Mujoco tasks, and $\mathcal{T}Q_{\theta_i} = r + \gamma \left(Q_{\theta_i}(s', a') - \beta \log \pi(a'|s') \right)$ when using independent targets in Equation 3 for AntMaze tasks. The policy is learned by optimizing the following loss function:

$$\mathcal{L}_\pi = \mathbb{E}_{(s, a) \sim \mathcal{D}} \left[\min_i Q_{\theta_i}(s, a) + \beta \log \pi_\phi(a|s) + \eta_3 D_J(\pi_\phi(\cdot|s) \parallel \pi_\phi(\cdot|\hat{s})) \right], \quad (7)$$

where ϕ represents the parameters of the policy network. In Equation 7, the first term maximizes the minimum of the ensemble Q -functions to obtain a conservative policy, the second term is the entropy regularization, and the third term is the smooth constraint. We remark that we maintain the same loss function throughout the O2O process, which is more elegant than previous O2O methods. The difference between the pre-training and the fine-tuning phase lies in the data sampled to estimate of the expectations in Equation 6 and Equation 7. In implementation, we also apply normalization to states, which is widely used in previous work (Fujimoto and Gu 2021; Raffin et al. 2021). This also helps to deal with the variations of states in the fine-tuning phase.

Algorithm 1: Robust Offline-to-Online RL algorithm

Require: ensemble Q -networks $\{Q_{\theta_i}\}_{i=1}^n$, target networks $\{Q_{\theta_i^-}\}_{i=1}^n$, and policy network π_ϕ .

- 1: // *Offline Pre-training*
- 2: **while** $t \leq T_1$ **do**
- 3: Sample mini batches from \mathcal{D} .
- 4: Calculate robustness regularization $\mathcal{L}_{\text{Qsmooth}}, \mathcal{L}_{\text{ood}}$.
- 5: Update Q -functions with Equation 6 and update target networks softly.
- 6: Update the policy with Equation 7.
- 7: **end while**
- 8: // *Online Fine-tuning*
- 9: **while** $t \leq T_2$ **do**
- 10: Interact with the online environment with π_ϕ .
- 11: Collect transitions into new buffer \mathcal{B} .
- 12: Sample batches from buffer \mathcal{B} .
- 13: Update Q -functions and the policy with $\mathcal{L}_Q, \mathcal{L}_\pi$.
- 14: **end while**

Theoretical Analysis

Our analyses are conducted in linear MDP assumption (Jin et al. 2020; Jin, Yang, and Wang 2021a), where the transition kernel and the reward function are linear in a given state-action feature $\phi(s, a)$. We estimate the value function by $Q(s, a) \approx \hat{w}^\top \phi(s, a)$. See the appendix for the details.

We start by considering the offline training stage where the value function is learned from $\mathcal{D}_{\text{offline}}$. According to the loss in Equation 6, the parameter \hat{w} can be solved by

$$\begin{aligned} \tilde{w}_{\text{offline}} = \min_{w \in \mathcal{R}^d} & \left[\sum_{i=1}^m (y_t^i - Q_w(s_t^i, a_t^i))^2 + \right. \\ & \left. \sum_{(\hat{s}, \hat{a}, \hat{y}) \sim \mathcal{D}_{\text{ood}}} (\hat{y} - Q_w(\hat{s}, \hat{a}))^2 + \right. \\ & \left. \sum_{i=1}^m \frac{1}{|\mathbb{B}_d(s_t^i, \epsilon)|} \sum_{(\hat{s}_t^i, \hat{s}_t^i, \hat{a}_t^i) \in \mathcal{D}_{\text{robust}}} (Q_w(s_t^i, a_t^i) - Q_w(\hat{s}_t^i, \hat{a}_t^i))^2 \right], \end{aligned} \quad (8)$$

where we denote $y = \hat{\mathcal{T}}Q$ and $\hat{y} = \hat{\mathcal{T}}^{\text{ood}}Q$ as the learning targets for simplicity. The three terms in Equation 8 correspond to TD-loss, OOD penalty, and smoothness constraints, respectively. For the clarity of notations, we explicitly define a dataset \mathcal{D}_{ood} for OOD sampling, and an adversarial dataset $\mathcal{D}_{\text{robust}}$ for the smoothness term. Following Least-Squares Value Iteration (LSVI) (Jin et al. 2020), the solution of Equation 8 takes the following form as

$$\tilde{w}_t = \tilde{\Lambda}_t^{-1} \left(\sum_{i=1}^m \phi(s_t^i, a_t^i) y_t^i + \sum_{(\hat{s}, \hat{a}, \hat{y}) \sim \mathcal{D}_{\text{ood}}} \phi(\hat{s}, \hat{a}) \hat{y} \right), \quad (9)$$

and the covariance matrix $\tilde{\Lambda}_t$ is

$$\tilde{\Lambda}_t = \tilde{\Lambda}_t^{\text{in}} + \tilde{\Lambda}_t^{\text{ood}} + \tilde{\Lambda}_t^{\text{robust}}, \quad (10)$$

where the first term $\tilde{\Lambda}_t^{\text{in}} = \sum_{i=1}^m \phi(s_t^i, a_t^i) \phi(s_t^i, a_t^i)^\top$ is calculated on in-distribution (i.e., in $\mathcal{D}_{\text{offline}}$) data, the second term is $\tilde{\Lambda}_t^{\text{ood}} = \sum_{\mathcal{D}_{\text{ood}}} \phi(\hat{s}_t, \hat{a}_t) \phi(\hat{s}_t, \hat{a}_t)^\top$ is calculated on

OOD samples (i.e., in \mathcal{D}_{ood}), and the third term is calculated on adversarial samples (i.e., in $\mathcal{D}_{\text{robust}}$), as $\tilde{\Lambda}_t^{\text{robust}} = \sum_{i=1}^m \frac{1}{|\mathbb{B}_d|} \sum_{(\hat{s}_t^i, \hat{s}_t^i, \hat{a}_t^i) \in \mathcal{D}_{\text{robust}}} [\phi(\hat{s}_t^i, \hat{a}_t^i) - \phi(s_t^i, a_t^i)] [\phi(\hat{s}_t^i, \hat{a}_t^i) - \phi(s_t^i, a_t^i)]^\top$.

For comparison, we consider a variant of RO2O without smoothness regularization. Following LSVI, the solution of this variant takes a similar form as Equation 9, but with a different covariance matrix as $\tilde{\Lambda}_t^{\text{in}} + \tilde{\Lambda}_t^{\text{ood}}$. The difference in covariance matrices originates from the additional adversarial samples in RO2O. We denote the dataset for RO2O as $\mathcal{D}_{\text{RO2O}} = \mathcal{D}_{\text{offline}} \cup \mathcal{D}_{\text{ood}} \cup \mathcal{D}_{\text{robust}}$, and for this variant as $\mathcal{D}_{\text{variant}} = \mathcal{D}_{\text{offline}} \cup \mathcal{D}_{\text{ood}}$ without smoothness constraints.

Following the theoretical framework in PEVI (Jin, Yang, and Wang 2021b), the sub-optimality gap of offline RL algorithms with uncertainty penalty is upper-bounded by the lower-confidence-bound (LCB) term, defined by

$$\Gamma^{\text{lc}}(s_t, a_t; \mathcal{D}) = \beta_t [\phi(s_t, a_t)^\top \Lambda_t^{-1} \phi(s_t, a_t)]^{1/2}, \quad (11)$$

where the form of Λ_t depends on the learned dataset (e.g., $\mathcal{D}_{\text{RO2O}}$ or $\mathcal{D}_{\text{variant}}$), and β_t is a factor. Then the following theorem shows our smoothness regularization leads to smaller uncertainties for arbitrary state-action pairs, especially for OOD samples (e.g., from online interactions).

Theorem 1. *Assuming that the size of adversarial samples $\mathbb{B}_d(s_t^i, \epsilon)$ is sufficient and the Jacobian matrix of $\phi(s, a)$ has full rank, the smoothness constraint leads to smaller uncertainty for $\forall (s^*, a^*) \in \mathcal{S} \times \mathcal{A}$, as*

$$\Gamma^{\text{lc}}(s^*, a^*; \mathcal{D}_{\text{RO2O}}) < \Gamma^{\text{lc}}(s^*, a^*; \mathcal{D}_{\text{variant}}), \quad (12)$$

where the covariance matrices for these two LCB terms are $\tilde{\Lambda}_t$ in Equation 10 and $\tilde{\Lambda}_t^{\text{in}} + \tilde{\Lambda}_t^{\text{ood}}$, respectively.

As an extreme example in tabular case, the uncertainty for a purely OOD (s^*, a^*) pair can be large as $\Gamma^{\text{lc}}(s^*, a^*; \mathcal{D}_{\text{variant}}) \rightarrow \infty$ without the smoothness term, while $\Gamma^{\text{lc}}(s^*, a^*; \mathcal{D}_{\text{RO2O}}) \leq \beta_t / \sqrt{\lambda}$ with $\lambda > 0$. As a result, RO2O is more robust to significant distribution shift theoretically. See appendix for the proof.

Then, for online fine-tuning with new data from $\mathcal{D}_{\text{online}}$, the following theorem shows RO2O can consistently reduce the sub-optimality gap with online fine-tuning, as

Theorem 2. *Under the same conditions as Theorem 1, with additional online experience in the fine-tuning stage, the sub-optimality gap holds for RO2O in linear MDPs, as*

$$\begin{aligned} \text{SubOpt}(\pi^*, \tilde{\pi}) & \leq \sum_{t=1}^T \mathbb{E}_{\pi^*} [\Gamma_i^{\text{lc}}(s_t, a_t; \mathcal{D}_{\text{RO2O}} \cup \mathcal{D}_{\text{online}})] \\ & \leq \sum_{t=1}^T \mathbb{E}_{\pi^*} [\Gamma_i^{\text{lc}}(s_t, a_t; \mathcal{D}_{\text{RO2O}})], \end{aligned} \quad (13)$$

where $\tilde{\pi}$ and π^* are the learned policy and the optimal policy in $\mathcal{D}_{\text{RO2O}} \cup \mathcal{D}_{\text{online}}$, respectively.

Theorem 4 shows that the optimality gap shrinks if the data coverage of π^* is better. See appendix for the proof. Considering a sub-optimal dataset is used in offline training, via interacting and learning in online fine-tuning, the agent is potential to obtain high-quality data to consistently reduce the sub-optimality and result in a near-optimal policy.

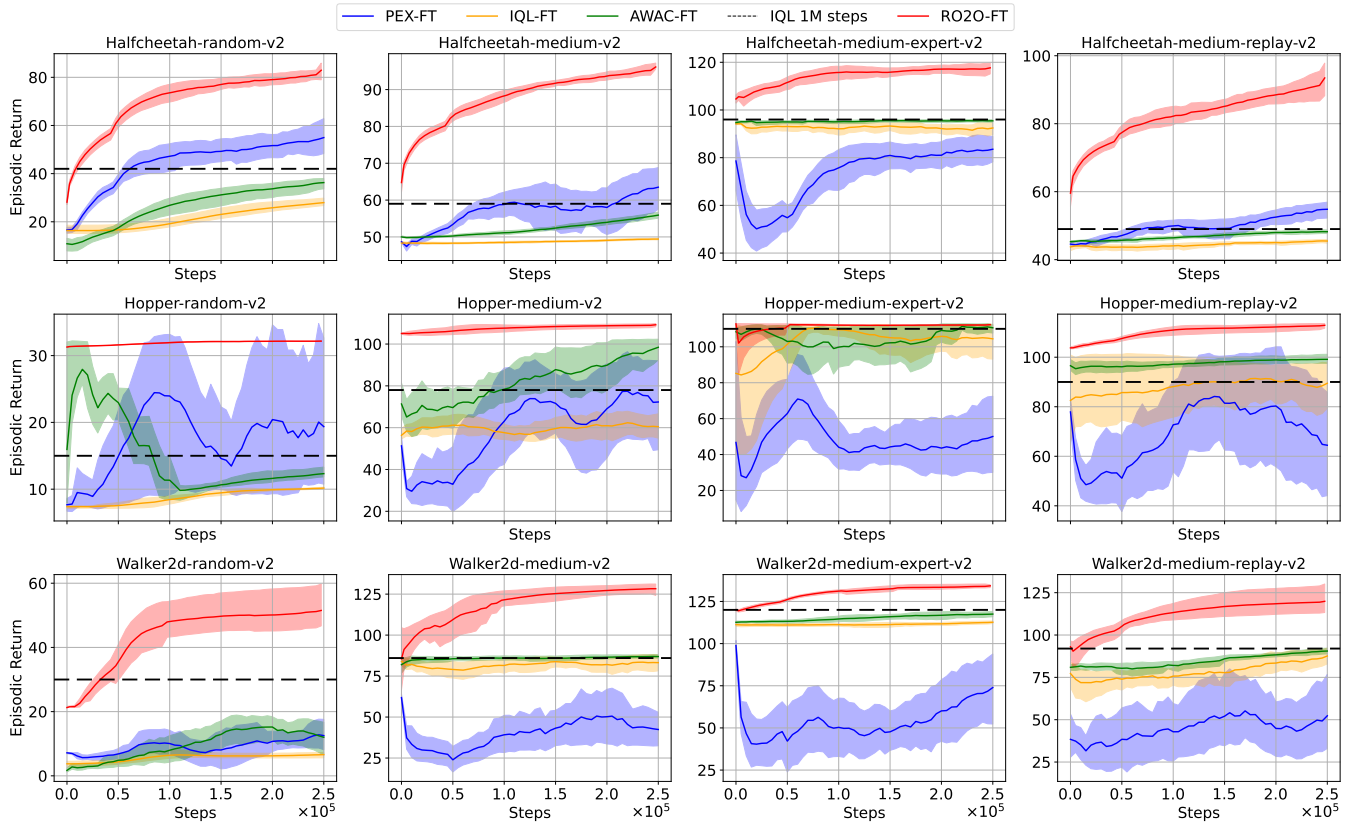


Figure 3: Fine-tuning performance Curves of different methods across three seeds on MuJoCo locomotion tasks. The mean and standard deviation are shown by the solid lines and the shaded areas, respectively.

Experiments

We present a comprehensive evaluation of RO2O in the context of the offline-to-online RL setting. Specifically, we investigate whether RO2O can perform favorable offline training and further policy improvement given limited interactions. We compare RO2O to existing offline RL algorithms in offline pertaining and also compare it to O2O algorithms in online adaptation. We also conduct ablation studies and visualizations to illustrate the effectiveness of our method.

Setups and Baselines

Our experiments are conducted on challenging environments from the D4RL (Fu et al. 2020) benchmark, specifically focusing on the Mujoco and AntMaze tasks. These environments are carefully selected to simulate real-world scenarios with limited data availability. We compare RO2O with the following RL algorithms: (i) PEX (Zhang, Xu, and Yu 2023): a recent O2O method that performs policy expansion and uses IQL for offline training. (ii) AWAC (Nair et al. 2020): an efficient algorithm employing advantage-weighted form actor-critic. (iii) IQL (Kostrikov, Nair, and Levine 2022): an algorithm that attempts to conduct in-sample learning and expected regression. For AntMaze tasks, we also compare RO2O with Cal-QL (Nakamoto et al. 2023), which calibrates Q -values within a reasonable range, and SPOT (Wu et al. 2022), which utilizes density regular-

ization to limit the difference between the learning strategy and the current strategy. More details about experiments and implementations are introduced in the appendix.

Environments	SPOT	IQL	Cal-QL	PEX	RO2O
antmaze-umaze	89 ± 5.29	77.0 ± 6.38	65.75 ± 4.03	87.33 ± 4.04	93.67 ± 5.77
antmaze-umaze-diverse	42.75 ± 5.32	65.24 ± 6.40	48.75 ± 4.43	58.67 ± 9.07	63.67 ± 8.02
antmaze-medium-diverse	74.25 ± 4.99	73.75 ± 6.30	1.25 ± 0.96	72.33 ± 5.13	91.67 ± 5.13
antmaze-medium-play	71.5 ± 8.43	66 ± 7.55	0.0 ± 0.0	68 ± 6.56	86.67 ± 3.06
antmaze-large-diverse	36.5 ± 17.62	30.25 ± 4.20	0.0 ± 0.0	45.67 ± 4.16	65.33 ± 5.71
antmaze-large-play	30.25 ± 17.91	42.0 ± 5.23	0.25 ± 0.5	51 ± 17.69	61.33 ± 9.82

Table 1: Offline performance on challenging AntMaze tasks.

Performance Comparisons

The comparisons are conducted on multiple offline datasets and tasks. For Mujoco locomotion tasks, we consider three environments, including halfcheetah, walker2d, and hopper, and different types of datasets, including random, medium, medium-replay, medium-expert, and expert datasets. Due to space limitations, we present the offline performance over all Mujoco tasks and the fine-tuning performance on expert datasets in the appendix. For AntMaze tasks, agents are pre-trained on six types of datasets with different complexity and quality. Table 1 reports the normalized scores using different methods across three seeds, where RO2O achieves the best performance on almost all tasks.

Fine-tuning performance on Mujoco locomotion tasks
Figure 3 illustrates the fine-tuning performance of different

methods on Mujoco locomotion tasks. Within limited online interactions, IQL and AWAC fail to achieve effective policy improvement, while PEX suffers from the performance drop. We speculate that it is due to the randomness of strategies expanded in the online phase, which could lead to a poor initial strategy and requires lots of interactions to improve its performance. In contrast, RO2O exhibits a significant improvement in performance during the fine-tuning process, and requires fewer steps to achieve the highest score. We also present the fine-tuning performance of IQL given 1M interacting steps, which is represented by the yellow dashed line in Figure 3. Compared with them, RO2O showcases comparable or better performance with 250K fine-tuning steps, indicating the efficiency and superiority.

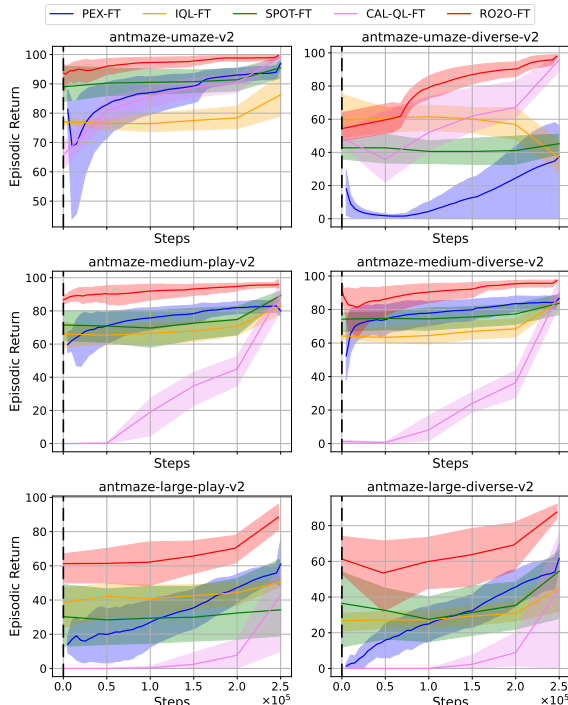


Figure 4: Fine-tuning performance curves of different methods across three seeds on Antmaze navigation tasks. The mean and standard deviation are shown by the solid lines and the shaded areas, respectively.

Fine-tuning performance on AntMaze navigation tasks
Figure 4 demonstrates the fine-tuning performance on AntMaze tasks. In the fine-tuning phase, IQL and SPOT achieve stable learning but limited improvement, while PEX suffers from a performance drop. Cal-QL rapidly enhances its performance from a poor initial policy, but cannot perform well in large scenarios. Different from these baseline methods, RO2O achieves significant improvement over all tasks within limited interactions.

Ablation Study and Visualization

We analyze the effects of the smoothness regularization and OOD sampling terms on the learning process. Specifically, we consider variants of RO2O without policy smoothing, Q -smoothing, or OOD penalty. We conduct the ablation stud-

ies on walker2d-medium and hopper-medium tasks. Figure 5 demonstrates the experimental results over 3 random seeds. In the offline process, we observe that OOD penalty is indispensable to prevent divergence caused by OOD actions. However, it becomes trivial in the online phase since new states or actions may lead to high values and better policies. We also find that policy smoothing and Q -smoothing are useful in the O2O process to obtain an effective improvement and mitigate the variance of performance.

To better understand the effective of RO2O in the O2O process, we compare the distribution of the offline states and the visited states in online interactions, as shown in Figure 6(left). The states are visualized via T-SNE. Meanwhile, we use brightness to represent the corresponding reward for each state, as shown in Figure 6(right). We find that, with consistent policy improvement in online fine-tuning, the agent can obtain high-quality (i.e., with high reward) online experiences that are different from the offline data. Such a phenomenon verifies our theoretical analysis in Theorem 4, where RO2O can consistently reduce the sub-optimality gap and improve the policy via online fine-tuning.

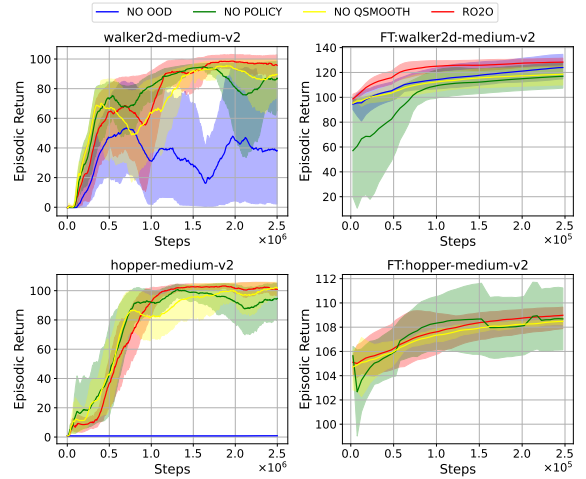


Figure 5: Offline (left column) and online performance (right column) when eliminating OOD penalty, policy smoothing, or Q -smoothing.

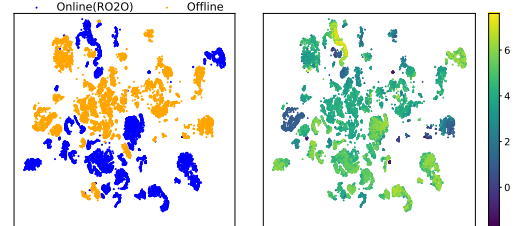


Figure 6: Visualization of the distribution of states (left) and rewards (right) from offline data and online experiences.

Conclusion

In this paper, we propose RO2O for offline-to-online RL by incorporating Q -ensembles and smoothness regularization.

By regularizing the smoothness of value and policy, RO2O achieve stable offline learning and effective policy improvement in online fine-tuning. Moreover, RO2O maintains the same architecture in the O2O process without specific modifications. Empirical results on Mujoco and AntMaze tasks demonstrate the effectiveness and superiority of RO2O. Future work may explore ways to perform O2O learning with domain gaps, including dynamics or reward differences.

Acknowledgments

This work is supported by the National Science Fund for Distinguished Young Scholars (Grant No.62025602), the National Natural Science Foundation of China (Grant Nos. 62306242, U22B2036, 11931915), Fok Ying-Tong Education Foundation China (No.171105), the Tencent Foundation, and XPLORER PRIZE.

References

An, G.; Moon, S.; Kim, J.-H.; and Song, H. O. 2021a. Uncertainty-based offline reinforcement learning with diversified q-ensemble. *Advances in neural information processing systems*, 34: 7436–7447.

An, G.; Moon, S.; Kim, J.-H.; and Song, H. O. 2021b. Uncertainty-based offline reinforcement learning with diversified q-ensemble. *Advances in neural information processing systems*, 34: 7436–7447.

Aytar, Y.; Pfaff, T.; Budden, D.; Paine, T.; Wang, Z.; and De Freitas, N. 2018. Playing hard exploration games by watching youtube. *Advances in neural information processing systems*, 31.

Bai, C.; Wang, L.; Yang, Z.; Deng, Z.-H.; Garg, A.; Liu, P.; and Wang, Z. 2022. Pessimistic Bootstrapping for Uncertainty-Driven Reinforcement Learning. In *International Conference on Learning Representations*.

Bojarski, M.; Del Testa, D.; Dworakowski, D.; Firner, B.; Flepp, B.; Goyal, P.; Jackel, L. D.; Monfort, M.; Muller, U.; Zhang, J.; et al. 2016. End to end learning for self-driving cars. *arXiv preprint arXiv:1604.07316*.

Chen, R. Y.; Sidor, S.; Abbeel, P.; and Schulman, J. 2017. Ucb exploration via q-ensembles. *arXiv preprint arXiv:1706.01502*.

Chen, X.; Wang, C.; Zhou, Z.; and Ross, K. W. 2021. Randomized Ensembled Double Q-Learning: Learning Fast Without a Model. In *International Conference on Learning Representations*.

Fu, J.; Kumar, A.; Nachum, O.; Tucker, G.; and Levine, S. 2020. D4rl: Datasets for deep data-driven reinforcement learning. *arXiv preprint arXiv:2004.07219*.

Fujimoto, S.; and Gu, S. S. 2021. A minimalist approach to offline reinforcement learning. *Advances in neural information processing systems*, 34: 20132–20145.

Fujimoto, S.; Hoof, H.; and Meger, D. 2018. Addressing function approximation error in actor-critic methods. In *International conference on machine learning*, 1587–1596. PMLR.

Ghasemipour, K.; Gu, S. S.; and Nachum, O. 2022. Why so pessimistic? estimating uncertainties for offline rl through ensembles, and why their independence matters. *Advances in Neural Information Processing Systems*, 35: 18267–18281.

Haarnoja, T.; Zhou, A.; Abbeel, P.; and Levine, S. 2018. Soft actor-critic: Off-policy maximum entropy deep reinforcement learning with a stochastic actor. In *International conference on machine learning*, 1861–1870. PMLR.

Hessel, M.; Modayil, J.; Van Hasselt, H.; Schaul, T.; Ostrovski, G.; Dabney, W.; Horgan, D.; Piot, B.; Azar, M.; and Silver, D. 2018. Rainbow: Combining improvements in deep reinforcement learning. In *Proceedings of the AAAI conference on artificial intelligence*, volume 32.

Jin, C.; Yang, Z.; Wang, Z.; and Jordan, M. I. 2020. Provably efficient reinforcement learning with linear function approximation. In *Conference on Learning Theory*, 2137–2143. PMLR.

Jin, Y.; Yang, Z.; and Wang, Z. 2021a. Is Pessimism Provably Efficient for Offline RL? In *International Conference on Machine Learning*, 5084–5096. PMLR.

Jin, Y.; Yang, Z.; and Wang, Z. 2021b. Is pessimism provably efficient for offline rl? In *International Conference on Machine Learning*, 5084–5096. PMLR.

Kiran, B. R.; Sobh, I.; Talpaert, V.; Mannion, P.; Al Sal lab, A. A.; Yogamani, S.; and Pérez, P. 2021. Deep reinforcement learning for autonomous driving: A survey. *IEEE Transactions on Intelligent Transportation Systems*, 23(6): 4909–4926.

Kostrikov, I.; Nair, A.; and Levine, S. 2022. Offline Reinforcement Learning with Implicit Q-Learning. In *International Conference on Learning Representations*.

Kumar, A.; Zhou, A.; Tucker, G.; and Levine, S. 2020. Conservative q-learning for offline reinforcement learning. *Advances in Neural Information Processing Systems*, 33: 1179–1191.

Lambert, N.; Wulfmeier, M.; Whitney, W.; Byravan, A.; Bloesch, M.; Dasagi, V.; Hertweck, T.; and Riedmiller, M. 2022. The challenges of exploration for offline reinforcement learning. *arXiv preprint arXiv:2201.11861*.

Lample, G.; and Chaplot, D. S. 2017. Playing FPS games with deep reinforcement learning. In *Proceedings of the AAAI Conference on Artificial Intelligence*, volume 31.

Lan, Q.; Pan, Y.; Fyshe, A.; and White, M. 2020. Maxmin q-learning: Controlling the estimation bias of q-learning. *arXiv preprint arXiv:2002.06487*.

Lee, K.; Laskin, M.; Srinivas, A.; and Abbeel, P. 2021. Sunrise: A simple unified framework for ensemble learning in deep reinforcement learning. In *International Conference on Machine Learning*, 6131–6141. PMLR.

Lee, S.; Seo, Y.; Lee, K.; Abbeel, P.; and Shin, J. 2022. Offline-to-online reinforcement learning via balanced replay and pessimistic q-ensemble. In *Conference on Robot Learning*, 1702–1712. PMLR.

Levine, S.; Kumar, A.; Tucker, G.; and Fu, J. 2020. Offline reinforcement learning: Tutorial, review, and perspectives on open problems. *arXiv preprint arXiv:2005.01643*.

Miotto, R.; Wang, F.; Wang, S.; Jiang, X.; and Dudley, J. T. 2018. Deep learning for healthcare: review, opportunities and challenges. *Briefings in bioinformatics*, 19(6): 1236–1246.

Mnih, V.; Kavukcuoglu, K.; Silver, D.; Rusu, A. A.; Veness, J.; Bellemare, M. G.; Graves, A.; Riedmiller, M.; Fidjeland, A. K.; Ostrovski, G.; et al. 2015. Human-level control through deep reinforcement learning. *nature*, 518(7540): 529–533.

Nair, A.; Gupta, A.; Dalal, M.; and Levine, S. 2020. Awac: Accelerating online reinforcement learning with offline datasets. *arXiv preprint arXiv:2006.09359*.

Nakamoto, M.; Zhai, Y.; Singh, A.; Mark, M. S.; Ma, Y.; Finn, C.; Kumar, A.; and Levine, S. 2023. Cal-ql: Calibrated offline rl pre-training for efficient online fine-tuning. *arXiv preprint arXiv:2303.05479*.

Osband, I.; Blundell, C.; Pritzel, A.; and Van Roy, B. 2016. Deep exploration via bootstrapped DQN. *Advances in neural information processing systems*, 29.

Prudencio, R. F.; Maximo, M. R.; and Colombini, E. L. 2023. A survey on offline reinforcement learning: Taxonomy, review, and open problems. *IEEE Transactions on Neural Networks and Learning Systems*.

Raffin, A.; Hill, A.; Gleave, A.; Kanervisto, A.; Ernestus, M.; and Dormann, N. 2021. Stable-Baselines3: Reliable Reinforcement Learning Implementations. *Journal of Machine Learning Research*, 22(268): 1–8.

Schulman, J.; Levine, S.; Abbeel, P.; Jordan, M.; and Moritz, P. 2015. Trust region policy optimization. In *International conference on machine learning*, 1889–1897. PMLR.

Schulman, J.; Wolski, F.; Dhariwal, P.; Radford, A.; and Klimov, O. 2017. Proximal policy optimization algorithms. *arXiv preprint arXiv:1707.06347*.

Schweighofer, K.; Dinu, M.-c.; Radler, A.; Hofmarcher, M.; Patil, V. P.; Bitto-Nemling, A.; Eghbal-zadeh, H.; and Hochreiter, S. 2022. A dataset perspective on offline reinforcement learning. In *Conference on Lifelong Learning Agents*, 470–517. PMLR.

Shen, Q.; Li, Y.; Jiang, H.; Wang, Z.; and Zhao, T. 2020. Deep reinforcement learning with robust and smooth policy. In *International Conference on Machine Learning*, 8707–8718. PMLR.

Silver, D.; Hubert, T.; Schrittwieser, J.; Antonoglou, I.; Lai, M.; Guez, A.; Lanctot, M.; Sifre, L.; Kumaran, D.; Graepel, T.; et al. 2018. A general reinforcement learning algorithm that masters chess, shogi, and Go through self-play. *Science*, 362(6419): 1140–1144.

Sinha, S.; Mandlekar, A.; and Garg, A. 2022. S4rl: Surprisingly simple self-supervision for offline reinforcement learning in robotics. In *Conference on Robot Learning*, 907–917. PMLR.

Tobin, J.; Fong, R.; Ray, A.; Schneider, J.; Zaremba, W.; and Abbeel, P. 2017. Domain randomization for transferring deep neural networks from simulation to the real world. In *2017 IEEE/RSJ international conference on intelligent robots and systems (IROS)*, 23–30. IEEE.

Uchendu, I.; Xiao, T.; Lu, Y.; Zhu, B.; Yan, M.; Simon, J.; Bennice, M.; Fu, C.; Ma, C.; Jiao, J.; et al. 2023. Jump-start reinforcement learning. In *International Conference on Machine Learning*, 34556–34583. PMLR.

Van der Maaten, L.; and Hinton, G. 2008. Visualizing data using t-SNE. *Journal of machine learning research*, 9(11).

Wang, Z.; Bapst, V.; Heess, N.; Mnih, V.; Munos, R.; Kavukcuoglu, K.; and de Freitas, N. 2016. Sample efficient actor-critic with experience replay. *arXiv preprint arXiv:1611.01224*.

Wu, J.; Wu, H.; Qiu, Z.; Wang, J.; and Long, M. 2022. Supported policy optimization for offline reinforcement learning. *Advances in Neural Information Processing Systems*, 35: 31278–31291.

Yang, L.; and Wang, M. 2019. Sample-optimal parametric Q-learning using linearly additive features. In *International Conference on Machine Learning*, 6995–7004. PMLR.

Yang, R.; Bai, C.; Ma, X.; Wang, Z.; Zhang, C.; and Han, L. 2022. Rorl: Robust offline reinforcement learning via conservative smoothing. *Advances in Neural Information Processing Systems*, 35: 23851–23866.

Yu, T.; Thomas, G.; Yu, L.; Ermon, S.; Zou, J. Y.; Levine, S.; Finn, C.; and Ma, T. 2020. Mopo: Model-based offline policy optimization. *Advances in Neural Information Processing Systems*, 33: 14129–14142.

Zhang, H.; Xu, W.; and Yu, H. 2023. Policy Expansion for Bridging Offline-to-Online Reinforcement Learning. In *The Eleventh International Conference on Learning Representations*.

Zhao, K.; Ma, Y.; Liu, J.; Zheng, Y.; and Meng, Z. 2023. Ensemble-based Offline-to-Online Reinforcement Learning: From Pessimistic Learning to Optimistic Exploration. *arXiv preprint arXiv:2306.06871*.

Zhao, Y.; Boney, R.; Ilin, A.; Kannala, J.; and Pajarin, J. 2022. Adaptive behavior cloning regularization for stable offline-to-online reinforcement learning. *arXiv preprint arXiv:2210.13846*.

APPENDIX

Theoretical Analysis

Background of Linear MDPs

Our theoretical derivations build on top of linear MDP assumptions. Least Squares Value Iteration (LSVI) is a classic method frequently used in the linear MDPs to calculate the closed-form solution. In linear MDPs (Jin et al. 2020), the transition dynamics and reward function take the following form, as

$$\mathbb{P}_t(s_{t+1} | s_t, a_t) = \langle \varphi(s_{t+1}), \phi(s_t, a_t) \rangle, \quad r(s_t, a_t) = v^\top \phi(s_t, a_t), \quad \forall (s_{t+1}, a_t, s_t) \in \mathcal{S} \times \mathcal{A} \times \mathcal{S}, \quad (14)$$

where the feature embedding $\phi : \mathcal{S} \times \mathcal{A} \mapsto \mathbb{R}^d$ is known. We further assume that the reward function $r : \mathcal{S} \times \mathcal{A} \mapsto [0, 1]$ is bounded and the feature is bounded by $\|\phi\|_2 \leq 1$. We consider the settings of $\gamma = 1$ in the following. Then for any policy π , the state-action value function is also linear to ϕ , as

$$Q^\pi(s_t, a_t) = w^\top \phi(s_t, a_t). \quad (15)$$

Given data $\mathcal{D}_m = \{s_t^i, a_t^i, r_t^i, s_{t+1}^i\}_{i \in [m]}$, the parameter of the w can be solved via LSVI algorithm, as

$$\hat{w}_t = \min_{w \in \mathbb{R}^d} \sum_{i=1}^m (\phi(s_t^i, a_t^i)^\top w - r(s_t^i, a_t^i) - V_{t+1}(s_{t+1}^i))^2 \quad (16)$$

where V_{t+1} is the estimated value function in the $(t+1)$ -th step. Following LSVI, the explicit solution to Equation 16 takes the form of

$$\hat{w}_t = \Lambda_t^{-1} \sum_{i=1}^m \phi(s_t^i, a_t^i) y_t^i, \quad \text{where } \Lambda_t = \sum_{i=1}^m \phi(s_t^i, a_t^i) \phi(s_t^i, a_t^i)^\top \quad (17)$$

is the feature covariance matrix of the state-action pairs in the offline dataset, and $y_t^i = r(s_t^i, a_t^i) + V_{t+1}(s_{t+1}^i)$ is the Bellman target in regression.

RO2O Algorithm in Linear MDPs

Then we consider the loss function of RO2O algorithm in offline learning, which contains temporal-difference (TD) error, smoothness loss, and OOD penalty. Converting the loss function in linear MDPs, the parameter \hat{w} in RO2O can be solved by

$$\begin{aligned} \tilde{w}_{\text{offline}} = \min_{w \in \mathbb{R}^d} & \left[\sum_{i=1}^m (y_t^i - Q_w(s_t^i, a_t^i))^2 + \sum_{(\hat{s}, \hat{a}, \hat{y}) \sim \mathcal{D}_{\text{ood}}} (\hat{y} - Q_w(\hat{s}, \hat{a}))^2 \right. \\ & \left. + \sum_{i=1}^m \frac{1}{|\mathbb{B}_d(s_t^i, \epsilon)|} \sum_{(\hat{s}_t^i, s_t^i, a_t^i) \in \mathcal{D}_{\text{robust}}} (Q_w(s_t^i, a_t^i) - Q_w(\hat{s}_t^i, a_t^i))^2 \right], \end{aligned} \quad (18)$$

where we denote $y = \hat{\mathcal{T}}Q$ and $\hat{y} = \hat{\mathcal{T}}^{\text{ood}}Q$ as the learning targets for simplicity. The three terms in Equation 18 correspond to TD-loss, OOD penalty, and smoothness constraints, respectively. For the clarity of notations, we explicitly define a dataset \mathcal{D}_{ood} for OOD sampling, and an adversarial dataset $\mathcal{D}_{\text{robust}}$ for the smoothness constraint. Following LSVI (Jin et al. 2020), the solution of Equation 18 takes the following form as

$$\tilde{w}_t = \tilde{\Lambda}_t^{-1} \left(\sum_{i=1}^m \phi(s_t^i, a_t^i) y_t^i + \sum_{(\hat{s}, \hat{a}, \hat{y}) \sim \mathcal{D}_{\text{ood}}} \phi(\hat{s}, \hat{a}) \hat{y} \right), \quad (19)$$

and the covariance matrix $\tilde{\Lambda}_t$ is

$$\begin{aligned} \tilde{\Lambda}_t &= \tilde{\Lambda}_t^{\text{in}} + \tilde{\Lambda}_t^{\text{ood}} + \tilde{\Lambda}_t^{\text{robust}} \\ &= \sum_{i=1}^m \phi(s_t^i, a_t^i) \phi(s_t^i, a_t^i)^\top + \sum_{\mathcal{D}_{\text{ood}}} \phi(\hat{s}_t, \hat{a}_t) \phi(\hat{s}_t, \hat{a}_t)^\top + \sum_{i=1}^m \frac{1}{|\mathbb{B}_d(s_t^i, \epsilon)|} \sum_{\mathcal{D}_{\text{robust}}} [\phi(\hat{s}_t^i, a_t^i) - \phi(s_t^i, a_t^i)] [\phi(\hat{s}_t^i, a_t^i) - \phi(s_t^i, a_t^i)]^\top \end{aligned} \quad (20)$$

where the first term $\tilde{\Lambda}_t^{\text{in}}$ is calculated on in-distribution (i.e., in $\mathcal{D}_{\text{offline}}$) data, the second term is $\tilde{\Lambda}_t^{\text{ood}}$ is calculated on OOD samples (i.e., in \mathcal{D}_{ood}), and the third term is calculated on adversarial samples (i.e., in $\mathcal{D}_{\text{robust}}$).

For comparison, we consider a variant of RO2O without smoothness regularization, and denote it as ‘variant’. The parameter of this variant can be solved by

$$\tilde{w}_{\text{variant}} = \min_{w \in \mathcal{R}^d} \left[\sum_{i=1}^m (y_t^i - Q_w(s_t^i, a_t^i))^2 + \sum_{(\hat{s}, \hat{a}, \hat{y}) \sim \mathcal{D}_{\text{ood}}} (\hat{y} - Q_w(\hat{s}, \hat{a}))^2 \right], \quad (21)$$

Following LSVI, the solution of this variant takes a similar form as Equation 19, but with a different covariance matrix as

$$\tilde{\Lambda}_t^{\text{variant}} = \tilde{\Lambda}_t^{\text{in}} + \tilde{\Lambda}_t^{\text{ood}}. \quad (22)$$

We remark that the difference in covariance matrices between RO2O and this variant originates from the additional adversarial samples from $\mathcal{D}_{\text{robust}}$ used in RO2O. We denote the dataset for RO2O as

$$\mathcal{D}_{\text{RO2O}} = \mathcal{D}_{\text{offline}} \bigcup \mathcal{D}_{\text{ood}} \bigcup \mathcal{D}_{\text{robust}},$$

and for this variant as

$$\mathcal{D}_{\text{variant}} = \mathcal{D}_{\text{offline}} \bigcup \mathcal{D}_{\text{ood}}$$

without smoothness constraints.

Effective of smoothness with LCB

Following the theoretical framework in PEVI (Jin, Yang, and Wang 2021b), the sub-optimality gap of offline RL algorithms with uncertainty penalty is upper-bounded by the lower-confidence-bound (LCB) term, defined by

$$\Gamma^{\text{lcb}}(s_t, a_t; \mathcal{D}) = \beta_t [\phi(s_t, a_t)^\top \Lambda_t^{-1} \phi(s_t, a_t)]^{1/2}, \quad (23)$$

which forms an uncertainty quantification with the covariance matrix Λ_i^{-1} given the dataset \mathcal{D}_i (Jin et al. 2020; Jin, Yang, and Wang 2021a), and the form of Λ_t depends on the learned dataset (e.g., $\mathcal{D}_{\text{RO2O}}$ or $\mathcal{D}_{\text{variant}}$). β_t is a factor. LCB measures the confidence interval of Q -function learned by the given dataset. Intuitively, $\Gamma_i^{\text{lcb}}(s, a)$ can be considered as a reciprocal pseudo-count of the state-action pair in the representation space.

In the following, we aim to show the smoothness regularization leads to smaller uncertainties for arbitrary state-action pairs, especially for OOD samples (e.g., from online interactions). We start by building a Lemma to show the covariance matrix $\tilde{\Lambda}_t^{\text{robust}}$ introduced by smoothness regularization calculated in $\mathcal{D}_{\text{robust}}$ is positive-definite.

Lemma 1. *Assuming that the size of adversarial samples $\mathbb{B}_d(s_t^i, \epsilon)$ is sufficient and the Jacobian matrix of $\phi(s, a)$ has full rank, then the covariance matrix $\tilde{\Lambda}_t^{\text{robust}}$ is positive-definite: $\tilde{\Lambda}_t^{\text{robust}} \succeq \lambda \cdot \mathbf{I}$ where $\lambda > 0$.*

Proof. For the $\tilde{\Lambda}_t^{\text{robust}}$ matrix (i.e., the third part in Eq. (10)), we denote the covariance matrix for a specific i as Φ_t^i . Then we have $\tilde{\Lambda}_t^{\text{ood-diff}} = \sum_{i=1}^m \Phi_t^i$. In the following, we discuss the condition of positive-definiteness of Φ_t^i . For the simplicity of notation, we omit the superscript and subscript of s_t^i and a_t^i for given i and t . Specifically, we define

$$\Phi_t^i = \frac{1}{|\mathbb{B}_d(s_t^i, \epsilon)|} \sum_{\hat{s}_j \sim \mathcal{D}_{\text{ood}}(s)} [\phi(\hat{s}_j, a) - \phi(s, a)] [\phi(\hat{s}_j, a) - \phi(s, a)]^\top,$$

where $j \in \{1, \dots, N\}$ indicates we sample $|\mathbb{B}_d(s_t^i, \epsilon)| = N$ perturbed states for each s . For a nonzero vector $y \in \mathbb{R}^d$, we have

$$\begin{aligned} y^\top \Phi_t^i y &= y^\top \left(\frac{1}{N} \sum_{j=1}^N (\phi(\hat{s}_j, a) - \phi(s, a)) (\phi(\hat{s}_j, a) - \phi(s, a))^\top \right) y \\ &= \frac{1}{N} \sum_{j=1}^N y^\top (\phi(\hat{s}_j, a) - \phi(s, a)) (\phi(\hat{s}_j, a) - \phi(s, a))^\top y \\ &= \frac{1}{N} \sum_{j=1}^N \left((\phi(\hat{s}_j, a) - \phi(s, a))^\top y \right)^2 \geq 0, \end{aligned} \quad (24)$$

where the last inequality follows from the observation that $(\phi(\hat{s}_j, a) - \phi(s, a))^\top y$ is a scalar. Then Φ_t^i is always positive semi-definite. In the following, we denote $z_j = \phi(\hat{s}_j, a) - \phi(s, a)$. Then we need to prove that the condition to make Φ_t^i positive definite is $\text{rank}[z_1, \dots, z_N] = d$, where d is the feature dimension. Our proof follows contradiction.

In Equation 24, when $y^\top \Phi_t^i y = 0$ with a nonzero vector y , we have $z_j^\top y = 0$ for all $j = 1, \dots, N$. Suppose the set $\{z_1, \dots, z_N\}$ spans \mathbb{R}^d , then there exist real numbers $\{\alpha_1, \dots, \alpha_N\}$ such that $y = \alpha_1 z_1 + \dots + \alpha_N z_N$. But we have $y^\top y = \alpha_1 z_1^\top y + \dots + \alpha_N z_N^\top y = \alpha_1 \times 0 + \dots + \alpha_N \times 0 = 0$, yielding that $y = \mathbf{0}$, which forms a contradiction. Hence, if the set $\{z_1, \dots, z_N\}$ spans \mathbb{R}^d , which is equivalent to $\text{rank}[z_1, \dots, z_N] = d$, then Φ_t^i is positive definite.

Under the given conditions, since the size of samples $\mathbb{B}_d(s_t^i, \epsilon)$ is sufficient and the neural network maintains useful variability to make the Jacobian matrix of $\phi(s, a)$ have full rank, it ensures that $\exists k \in [1, m]$, for any nonzero vector $y \in \mathbb{R}^d$, $y^\top \Phi_t^k y > 0$. We have $y^\top \tilde{\Lambda}_t^{\text{robust}} y = \sum_{i=1}^m y^\top \Phi_t^i y \geq y^\top \Phi_t^k y > 0$. Therefore, $\tilde{\Lambda}_t^{\text{robust}}$ is positive definite, which concludes our proof. \square

Recall the covariance matrix of the variant algorithm without smoothness constraint is $\tilde{\Lambda}_t^{\text{variant}} = \tilde{\Lambda}_t^{\text{in}} + \tilde{\Lambda}_t^{\text{ood}}$, and RO2O has a covariance matrix as $\tilde{\Lambda}_t = \tilde{\Lambda}_t^{\text{variant}} + \tilde{\Lambda}_t^{\text{robust}}$, we have the following corollary based on Lemma 1.

Theorem 3 (restate). *Assuming that the size of adversarial samples $\mathbb{B}_d(s_t^i, \epsilon)$ is sufficient and the Jacobian matrix of $\phi(s, a)$ has full rank, the smoothness constraint leads to smaller uncertainty for $\forall (s^*, a^*) \in \mathcal{S} \times \mathcal{A}$, as*

$$\Gamma^{\text{lcb}}(s^*, a^*; \mathcal{D}_{\text{RO2O}}) < \Gamma^{\text{lcb}}(s^*, a^*; \mathcal{D}_{\text{variant}}), \quad (25)$$

where the covariance matrices for these two LCB terms are $\tilde{\Lambda}_t$ in Equation 20 and $\tilde{\Lambda}_t^{\text{in}} + \tilde{\Lambda}_t^{\text{ood}}$, respectively.

Proof. According to Lemma 1, since $\Lambda_t^{\text{robust}}$ is positive-definite, we have $\Lambda_t^{\text{robust}} \succeq \lambda I$ with a factor $\lambda > 0$. Meanwhile, the factor λ can be large if we have sufficient adversarial samples and also with large variability in adversarial samples. By assuming $\tilde{\Lambda}_t^{\text{in}} + \tilde{\Lambda}_t^{\text{ood}}$ is positive definite and leveraging the properties of generalized Rayleigh quotient, we have

$$\begin{aligned} \frac{\phi^\top (\tilde{\Lambda}_t^{\text{variant}})^{-1} \phi}{\phi^\top (\tilde{\Lambda}_t^{\text{variant}} + \tilde{\Lambda}_t^{\text{robust}})^{-1} \phi} &\geq \lambda_{\min}((\tilde{\Lambda}_t^{\text{variant}} + \tilde{\Lambda}_t^{\text{robust}})(\tilde{\Lambda}_t^{\text{variant}})^{-1}) \\ &= \lambda_{\min}(I + (\tilde{\Lambda}_t^{\text{robust}})(\tilde{\Lambda}_t^{\text{variant}})^{-1}) = 1 + \lambda_{\min}((\tilde{\Lambda}_t^{\text{robust}})(\tilde{\Lambda}_t^{\text{variant}})^{-1}). \end{aligned} \quad (26)$$

Since $\tilde{\Lambda}_t^{\text{robust}}$ and $(\tilde{\Lambda}_t^{\text{variant}})^{-1}$ are both positive definite, the eigenvalues of $\tilde{\Lambda}_t^{\text{robust}}(\tilde{\Lambda}_t^{\text{variant}})^{-1}$ are all positive: $\lambda_{\min}((\tilde{\Lambda}_t^{\text{robust}})(\tilde{\Lambda}_t^{\text{variant}})^{-1}) > 0$, where $\lambda_{\min}(\cdot)$ is the minimum eigenvalue.

Recall the uncertainty is calculated as $\Gamma^{\text{lcb}}(s_t, a_t; \mathcal{D}) = \beta_t [\phi(s_t, a_t)^\top \Lambda_t^{-1} \phi(s_t, a_t)]^{1/2}$. Then for $\forall \phi(s^*, a^*)$, we have

$$\phi(s^*, a^*)^\top (\tilde{\Lambda}_t^{\text{variant}})^{-1} \phi(s^*, a^*) > \phi(s^*, a^*)^\top (\tilde{\Lambda}_t^{\text{variant}} + \tilde{\Lambda}_t^{\text{robust}})^{-1} \phi(s^*, a^*) = \phi(s^*, a^*)^\top (\tilde{\Lambda}_t)^{-1} \phi(s^*, a^*), \quad (27)$$

which means that $\Gamma^{\text{lcb}}(s^*, a^*; \mathcal{D}_{\text{variant}}) > \Gamma^{\text{lcb}}(s^*, a^*; \mathcal{D}_{\text{RO2O}})$ and concludes our proof. \square

As an extreme case in tabular MDPs where the states and actions are finite, the LCB-penalty takes a simpler form. Specifically, we consider the joint state-action space $D = |\mathcal{S}| \times |\mathcal{A}|$. Then j -th state-action pair can be encoded as a one-hot vector as $\phi(s, a) \in \mathbb{R}^D$, where $j \in [0, D - 1]$. By considering the tabular MDP as a special case of the linear MDP (Yang and Wang 2019; Jin et al. 2020), we define

$$\phi(s_j, a_j) = \begin{bmatrix} 0 \\ \vdots \\ 1 \\ \vdots \\ 0 \end{bmatrix} \in \mathbb{R}^D, \quad \phi(s_j, a_j) \phi(s_j, a_j)^\top = \begin{bmatrix} 0 & \dots & 0 & \dots & 0 \\ \vdots & \ddots & & & \vdots \\ 0 & \dots & 1 & \dots & 0 \\ \vdots & & & \ddots & \vdots \\ 0 & \dots & 0 & \dots & 0 \end{bmatrix} \in \mathbb{R}^{D \times D}, \quad (28)$$

where the value of $\phi(s_j, a_j)$ is 1 at the j -th entry and 0 elsewhere. Then the matrix $\Lambda_j = \sum_{i=0}^m \phi(s_j^i, a_j^i) \phi(s_j^i, a_j^i)^\top$ is a specific covariance matrix based on the learned datasets. It takes the form of

$$\Lambda_j = \begin{bmatrix} n_0 & 0 & \dots & 0 \\ 0 & n_1 & \dots & 0 \\ \vdots & \ddots & \ddots & \vdots \\ 0 & \dots & n_j & 0 \\ \vdots & & & \vdots \\ 0 & \dots & \dots & n_{d-1} \end{bmatrix}, \quad (29)$$

where the j -th diagonal element of Λ_j is the corresponding counts for state-action (s_j, a_j) , i.e.,

$$n_j = N_{s_j, a_j}.$$

It thus holds that

$$[\phi(s_j, a_j)^\top \Lambda_j^{-1} \phi(s_j, a_j)]^{1/2} = \frac{1}{\sqrt{N_{s_j, a_j}}}, \quad (30)$$

For the variant algorithm of RO2O in Equation 21, since the value function is learned from $\mathcal{D}_{\text{variant}}$, the counting function also counts from this dataset. However, without any constraints, the count for a purely OOD state-action pair (s^*, a^*) can approach zero, and thus $\Gamma^{\text{lcb}}(s^*, a^*; \mathcal{D}_{\text{variant}}) \rightarrow \infty$ according to Equation 30. In contrast, as we proved in Lemma 1, the covariance matrix $\tilde{\Lambda}_t^{\text{robust}}$ for smoothness constraints is positive-definite as $\tilde{\Lambda}_t^{\text{robust}} \succeq \lambda \cdot \mathbf{I}$ where $\lambda > 0$. Then the covariance matrix for RO2O as $\tilde{\Lambda}_t \succeq \lambda \cdot \mathbf{I}$ since $\tilde{\Lambda}_t = \tilde{\Lambda}_t^{\text{variant}} + \tilde{\Lambda}_t^{\text{robust}}$. Then, we have $[\phi(s_j, a_j)^\top \Lambda_j^{-1} \phi(s_j, a_j)]^{1/2} < 1/\sqrt{\lambda}$ and thus $\Gamma^{\text{lcb}}(s^*, a^*; \mathcal{D}_{\text{RO2O}}) \leq \beta_t/\sqrt{\lambda}$ with $\lambda > 0$. As a result, RO2O is more robust to significant distribution shift theoretically.

Sub-optimality gap of RO2O

To quantify the sub-optimality gap, we start by the following lemma to show the ensemble Q -networks used in RO2O can recover the LCB term in linear MDPs.

Lemma 2 (Equivalence between LCB-penalty and Ensemble Uncertainty). *We assume that the noise in linear regression follows the standard Gaussian, then it holds for the posterior of w given \mathcal{D}_i that*

$$\mathbb{V}_{\hat{w}}[Q_i(s, a)] = \mathbb{V}_{\hat{w}}(\phi(s, a)^\top \hat{w}) = \phi(s, a)^\top \Lambda^{-1} \phi(s, a), \quad \forall (s, a) \in \mathcal{S} \times \mathcal{A}. \quad (31)$$

Proof. We refer to the proof in Lemma 1 of Bai et al. (2022). \square

In RO2O, we choose the minimum value among ensemble Q -networks (i.e., $\min Q_i$) as the learning target, which is equivalent to the uncertainty penalty as *i.e.*, $\bar{Q} - \alpha \sqrt{\mathbb{V}(Q_i)}$ with a specific α (An et al. 2021a). The following theorem shows RO2O can consistently reduce the sub-optimality gap with online fine-tuning.

Theorem 4. *Under the same conditions as Theorem 3, with additional online experience in the fine-tuning stage, the sub-optimality gap holds for RO2O in linear MDPs, as*

$$\begin{aligned} \text{SubOpt}(\pi^*, \tilde{\pi}) &\leq \sum_{t=1}^T \mathbb{E}_{\pi^*} [\Gamma^{\text{lcb}}(s_t, a_t; \mathcal{D}_{\text{RO2O}} \bigcup \mathcal{D}_{\text{online}})] \\ &\leq \sum_{t=1}^T \mathbb{E}_{\pi^*} [\Gamma^{\text{lcb}}(s_t, a_t; \mathcal{D}_{\text{RO2O}})], \end{aligned} \quad (32)$$

where $\tilde{\pi}$ and π^* are the learned policy and the optimal policy in $\mathcal{D}_{\text{RO2O}} \bigcup \mathcal{D}_{\text{online}}$, respectively.

Proof. Based on the LSVI solution of $\tilde{w}_{\text{offline}}$, we consider importing additional dataset $\mathcal{D}_{\text{finetune}}$ in online interactions. Following a similar solution procedure as in Equation 18 via LSVI, we obtain the solution of RO2O with online dataset as

$$\hat{w}_t^{\text{RO2O}} = (\tilde{\Lambda}_t^{\text{RO2O}})^{-1} \left(\sum_{(s, a, y) \sim \mathcal{D}_{\text{offline}} \bigcup \mathcal{D}_{\text{finetune}}} \phi(s, a) y + \sum_{(\hat{s}, \hat{a}, \hat{y}) \sim \hat{\mathcal{D}}_{\text{ood}}} \phi(\hat{s}, \hat{a}) \hat{y} \right), \quad (33)$$

where $\hat{\mathcal{D}}_{\text{ood}}$ is a new OOD dataset that contains OOD samples of both the offline and online data. The new covariance matrix $\tilde{\Lambda}_t^{\text{RO2O}}$ is calculated on samples in both online and offline data,

$$\tilde{\Lambda}_t^{\text{RO2O}} = \tilde{\Lambda}_t + \tilde{\Lambda}_{\text{online}}$$

$$= \sum_{\mathcal{D}_{\text{offline}} \bigcup \mathcal{D}_{\text{finetune}}} \phi(s_t^i, a_t^i) \phi(s_t^i, a_t^i)^\top + \sum_{\hat{\mathcal{D}}_{\text{ood}}} \phi(\hat{s}_t, \hat{a}_t) \phi(\hat{s}_t, \hat{a}_t)^\top + \sum_{i=1}^m \frac{1}{|\mathbb{B}_d(s_t^i, \epsilon)|} \sum_{\hat{\mathcal{D}}_{\text{robust}}} [\phi(\hat{s}_t^i, a_t^i) - \phi(s_t^i, a_t^i)] [\phi(\hat{s}_t^i, a_t^i) - \phi(s_t^i, a_t^i)]^\top, \quad (34)$$

where each term is calculated on both the offline dataset and online-finetuning dataset since the proposed RO2O algorithm does not change the learning objective in the offline-to-online process. We denote the total data used in online fine-tuning as $\mathcal{D}_{\text{online}}$, which contains the $\mathcal{D}_{\text{finetune}}$ collected in interacting with the environment, the additional adversarial samples, and the OOD samples that are constructed based on $\mathcal{D}_{\text{finetune}}$. Then, $\tilde{\Lambda}_t^{\text{RO2O}}$ is the covariance matrix of samples from both offline and online datasets, *i.e.*, $\mathcal{D}_{\text{RO2O}} \bigcup \mathcal{D}_{\text{online}}$.

According to the theoretical framework of pessimistic value-iteration (Jin, Yang, and Wang 2021a), value iteration with LCB-based uncertainty penalty is provable efficient in offline RL. Based on the covariance matrix of RO2O, the LCB-term of RO2O learning in offline pre-training and online-fine-tuning are

$$\Gamma^{\text{lcb}}(s_t, a_t; \mathcal{D}_{\text{RO2O}}) = \beta_t [\phi(s_t, a_t)^\top (\tilde{\Lambda}_t)^{-1} \phi(s_t, a_t)]^{1/2}, \quad (35)$$

$$\text{and } \Gamma^{\text{lcb}}(s_t, a_t; \mathcal{D}_{\text{RO2O}} \bigcup \mathcal{D}_{\text{online}}) = \beta_t [\phi(s_t, a_t)^\top (\tilde{\Lambda}_t^{\text{RO2O}})^{-1} \phi(s_t, a_t)]^{1/2}, \quad (36)$$

respectively, where $\tilde{\Lambda}_t^{\text{RO2O}}$ is defined in Equation 34. According to the definition of ξ -uncertainty quantifier (Jin et al. 2020), $\Gamma^{\text{lcb}}(s_t, a_t; \mathcal{D}_{\text{RO2O}} \bigcup \mathcal{D}_{\text{online}})$ also forms a valid ξ -uncertainty quantifier under mild assumptions (Yang et al. 2022). According to Jin, Yang, and Wang (2021a), since $\Gamma^{\text{lcb}}(s_t, a_t; \mathcal{D}_{\text{RO2O}})$ is a valid ξ -uncertainty quantifier, the first inequality of Equation 32 holds in quantifying the sub-optimality gap. Further, since $\tilde{\Lambda}_t^{\text{RO2O}} \succeq \tilde{\Lambda}_t$ according to Equation 34, we have $\Gamma^{\text{lcb}}(s_t, a_t; \mathcal{D}_{\text{RO2O}} \bigcup \mathcal{D}_{\text{online}}) \leq \Gamma^{\text{lcb}}(s_t, a_t; \mathcal{D}_{\text{RO2O}})$ by following Equation 36 and 35, which concludes our proof. \square

Environmental Settings

In this section, we introduce more details of the experimental environments.

MuJoCo Locomotion We conduct experiments on three MuJoCo locomotion tasks from D4RL(Fu et al. 2020), namely HalfCheetah, Walker2d, and Hopper. The goal of each task is to move forward as far as possible without falling, while keeping the control cost minimal. For each task, we consider four types of datasets. The random datasets are generated by random policies, while the medium datasets contain trajectories collected by medium-level policies. The medium-replay datasets encompass all samples collected during the training of a medium-level agent from scratch. In the case of the medium-expert datasets, half of the data comprises rollouts from medium-level policies, while the other half consists of rollouts from expert-level policies. We utilize the v2 version of each dataset. For offline phase, We train agents for 2.5M gradient steps over all datasets with an ensemble size of $N = 10$. Then we run online fine-tuning for an additional 250k environment interactions.

Antmaze We also evaluate our method on the Antmaze navigation tasks that involve controlling an 8-DoF ant quadruped robot to navigate through mazes and reach a desired goal. The agent receives binary rewards based on whether it successfully reaches the goal or not. We study each method using the following datasets from D4RL (Fu et al. 2020): large-diverse, large-play, medium-diverse, medium-play, umaze-diverse, and umaze. The difference between diverse and play datasets is the optimality of the trajectories they contain. The diverse datasets consist of trajectories directed towards random goals from random starting points, whereas the play datasets comprise trajectories directed towards specific locations that may not necessarily correspond to the goal. We use the v2 version of each dataset. For offline phase, We train agents for 1M gradient steps over all datasets with an ensemble size of $N = 10$. Then we run online fine-tuning for an additional 250K environment interactions.

Implementation Details

In this section, we introduce implementation details and hyper-parameters for each task.

MuJoCo Locomotion We select PEX, AWAC and IQL as our baselines in mujoco locomotion tasks. For AWAC and IQL, we use the implementation provided by: <https://github.com/tinkoff-ai/CORL> with default hyperparameters. For PEX, we use the open-source code of the original paper provided by: <https://github.com/Haichao-Zhang/PEX>. We list the basic hyperparameters for these methods in Table 2. To compare the fine-tuning performance of the algorithms under limited online interactions, we reduce the number of online interaction steps from the previous 1M to 250k. All the hyper-parameters used in RO2O for the benchmark experiments are listed in Table 3. η_1 , η_2 , η_3 indicate the coefficient of the Q network smoothing loss $\mathcal{L}_{Q\text{smooth}}$, ood loss \mathcal{L}_{ood} and the policy smoothing loss $\mathcal{L}_{\text{policy}}$, respectively, where η_1 maintains a constant value of 0.0001, η_2 is tuned within $\{0.0, 0.1, 0.5\}$ and η_3 is searched in $\{0.1, 1.0\}$. Additionally, for the above three losses, we construct a perturbation set $\mathbb{B}_d(s, \epsilon) = \{\hat{s} : d(s, \hat{s}) \leq \epsilon\}$ by setting different epsilons ϵ . We denote the perturbation scales for the Q value functions, the policy, and the OOD loss as $\epsilon_Q, \epsilon_P, \epsilon_{\text{ood}}$. τ is set to control the weight of $\mathcal{L}_{Q\text{smooth}}$ which maintains a constant value of 0.2. The number of sampled perturbed observations n is set for tuning within $\{10, 20\}$. And α is set to control the pessimistic degree of \mathcal{L}_{ood} during the pre-trained phase. Moreover, discarding offline data buffer is adopted in RO2O, which exhibits benefits for stable transfer in our experiments and mitigates the distributional shift.

Hyper-parameters	PEX	AWAC	IQL	RO2O
Policy learning rate	3e-4	3e-4	3e-4	3e-4
Critic learning rate	3e-4	3e-4	3e-4	3e-4
Alpha learning rate	-	-	-	3e-4
Value learning rate	3e-4	-	3e-4	-
Activations	RELU	RELU	RELU	RELU
Ensemble size	2	2	2	10
Batch size	256	256	256	256
Optimizer	Adam	Adam	Adam	Adam
Discount factor γ	0.99	0.99	0.99	0.99

Table 2: Hyperparameters used in the D4RL experiments.

Antmaze We select PEX, SPOT and Cal-ql as our baselines in antmaze navigation tasks. For SPOT and Cal-ql, we use the implementation provided by: <https://github.com/tinkoff-ai/CORL> with default hyperparameters. We directly used the experimental results provided by CORL in weight & bias for comparison. For PEX, we use the open-source code of the original paper provided by: <https://github.com/Haichao-Zhang/PEX>. To compare the fine-tuning performance of the algorithms under limited online interactions, we reduce the number of online interaction steps from the previous 1M to 250k. We found that incorporating behavior cloning (BC) during the offline pre-training phase of the AntMaze task can effectively improve model performance. Additionally, making appropriate adjustments to BC during the online fine-tuning stage for certain tasks can also enhance the algorithm’s performance and stability. And we transform AntMaze rewards according to $4(r - 0.5)$ as per MSG(Ghasemipour,

Task Name	η_1	η_2	η_3	ϵ_Q	ϵ_P	ϵ_{ood}	τ	n	α
halfcheetah-random halfcheetah-medium halfcheetah-medium-replay halfcheetah-medium-expert halfcheetah-expert	0.0001	0.0	0.1	0.001	0.001	0.00	0.2	20	0
				0.001	0.001			10	
				0.001	0.001			10	
				0.001	0.001			10	
				0.005	0.005			10	
hopper-random hopper-medium hopper-medium-replay hopper-medium-expert hopper-expert	0.0001	0.5	0.1	0.005	0.005	0.01	0.2	20	$1.5 \rightarrow 1.0 (1e^{-6})$ $2.0 \rightarrow 0.1 (1e^{-6})$ $0.1 \rightarrow 0.0 (1e^{-6})$ $3.0 \rightarrow 1.0 (1e^{-6})$ $4.0 \rightarrow 1.0 (1e^{-6})$
walker2d-random walker2d-medium walker2d-medium-replay walker2d-medium-expert walker2d-expert	0.0001	0.5	1.0	0.005	0.005	0.01	0.2	20	$5.0 \rightarrow 0.5 (1e^{-5})$ $1.0 \rightarrow 0.1 (5e^{-7})$ $0.1 \rightarrow 0.1 (0.0)$ $0.1 \rightarrow 0.1 (0.0)$ $1.0 \rightarrow 0.5 (1e^{-6})$

Table 3: Hyper-parameters of RO2O for the MuJoCo domains.

Task Name	η_2	η_3	ϵ_P	ϵ_{ood}	n	policy objective	$\beta_{\text{BC, off}}$	$\beta_{\text{BC, on}}$	α
umaze umaze-diverse medium-play medium-diverse large-play large-diverse	1.0	0.3	0.005	0.01	20	LCB	5	5	$1.0 \rightarrow 1.0 (0.0)$
		0.3				LCB	10	20	$2.0 \rightarrow 2.0 (0.0)$
		0.3				LCB	2	2	$1.0 \rightarrow 1.0 (0.0)$
		0.3				LCB	4	4	$2.0 \rightarrow 1.0 (1e^{-6})$
		0.5				Min	2	8	$2.0 \rightarrow 1.0 (1e^{-6})$
		0.3				Min	2	8	$1.0 \rightarrow 1.0 (0.0)$

Table 4: Hyper-parameters of RO2O for the AntMaze domains.

Gu, and Nachum 2022) or CQL(Kumar et al. 2020). All the hyper-parameters used in RO2O for the benchmark experiments are listed in Table 4. $\beta_{\text{BC, off}}$ and $\beta_{\text{BC, on}}$ indicate the weight of BC regularization on policy networks during offline pre-training and online fine-tuning, respectively. The LCB policy objective and ‘Min’ policy objective represent optimizing the policy network using $\text{Mean}(Q_{\theta_i}(s, a)) - \text{Std}(Q_{\theta_i}(s, a))$ or $\min_i Q_{\theta_i}(s, a)$, respectively. And the meanings of other parameters remain consistent with Table 3 under the Mujoco tasks.

Additional Experimental Results

Offline performance on MuJoCo locomotion tasks We evaluate the performance of each method on Mujoco locomotion tasks, which include three environments: Halfcheetah, Walker2d, and Hopper. Different types of datasets are selected for offline pre-training, including random, medium, medium-replay, medium-expert, and expert datasets. We also compare with SAC-N (An et al. 2021b), which is an off-policy RL algorithm based on SAC by increasing the number of Q-network. Table 5 reports the offline performance of the average normalized score across three seeds. Compared to other algorithms, RO2O has certain superiority in the offline training phase.

Fine-tuning performance on expert datasets Figure 7 shows the normalized return curves of different methods on Mujoco expert datasets. We can observe that RO2O achieves the highest performance in all methods during the online fine-tuning phase with limited steps. Compared to AWAC and IQL, RO2O demonstrates significant performance improvements in the halfcheetah-expert-v2 and achieves superior performance on the walker-expert-v2 and hopper-expert-v2. For PEX, due to the unpredictability of the new strategies extended in the online phase, which may lead to choosing a weaker beginning strategy and necessitating additional environmental interaction to increase its performance, performance drops are noticeable on certain tasks. Within the limited number of fine-tuning steps, PEX doesn’t demonstrate superior performance.

Environments	PEX	AWAC	IQL	SAC-N	RO2O
halfcheetah-random	16.6 ± 1.21	10.88 ± 2.70	16.36 ± 1.94	28.0 ± 0.9	27.53 ± 0.32
halfcheetah-medium	48.67 ± 0.15	50.00 ± 0.27	48.33 ± 0.35	67.5 ± 1.2	66.08 ± 0.45
halfcheetah-medium-replay	44.57 ± 0.47	45.28 ± 0.31	43.75 ± 0.97	63.9 ± 0.8	60.89 ± 1.01
halfcheetah-medium-expert	78.9 ± 11.77	94.73 ± 0.64	94.19 ± 0.30	107.1 ± 2.0	104.73 ± 2.07
halfcheetah-expert	91.2 ± 4.43	97.57 ± 0.94	97.11 ± 0.19	105.2 ± 2.6	104.08 ± 1.66
walker2d-random	7.17 ± 0.23	1.70 ± 0.71	3.75 ± 0.89	21.7 ± 0.0	21.6 ± 0.03
walker2d-medium	61.87 ± 2.06	84.24 ± 1.15	83.96 ± 2.68	87.9 ± 0.2	103.25 ± 1.67
walker2d-medium-replay	38.4 ± 13.36	80.92 ± 1.70	77.28 ± 7.45	78.7 ± 0.7	93.05 ± 4.74
walker2d-medium-expert	98.8 ± 4.78	112.62 ± 0.66	111.24 ± 0.92	116.7 ± 0.4	120.01 ± 0.70
walker2d-expert	103.13 ± 6.69	91.66 ± 35.78	112.67 ± 0.21	107.4 ± 2.4	112.84 ± 3.42
hopper-random	7.67 ± 0.95	15.95 ± 13.94	7.38 ± 0.21	31.3 ± 0.0	31.35 ± 0.0
hopper-medium	51.3 ± 5.07	71.33 ± 8.80	56.33 ± 2.83	100.3 ± 0.3	104.95 ± 0.03
hopper-medium-replay	77.9 ± 5.77	96.56 ± 2.23	82.55 ± 17.57	101.8 ± 0.5	103.77 ± 0.47
hopper-medium-expert	46.73 ± 48.88	108.36 ± 3.12	85.21 ± 39.43	110.1 ± 0.3	112.69 ± 0.02
hopper-expert	102.27 ± 6.11	103.88 ± 8.98	100.36 ± 9.96	110.3 ± 0.3	112.31 ± 0.01

Table 5: Offline performance on MuJoCo locomotion tasks.

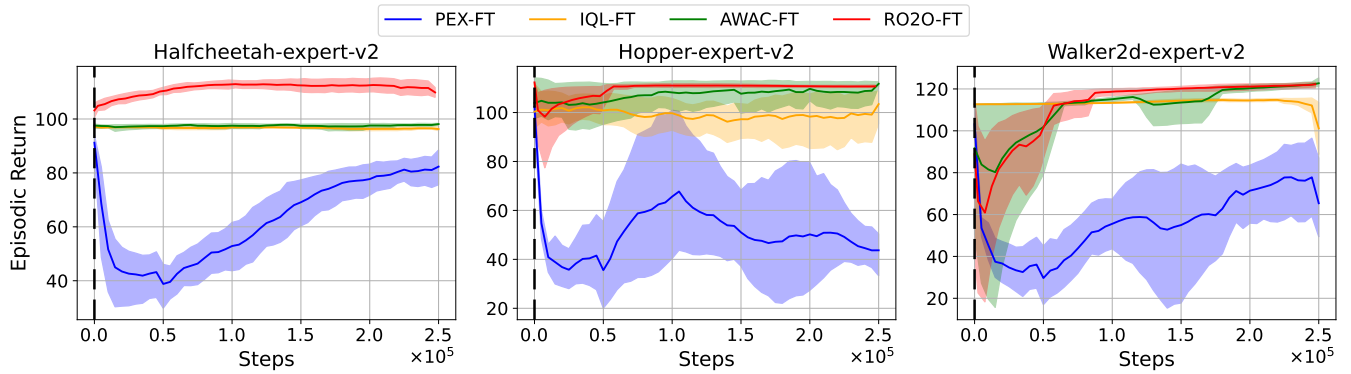


Figure 7: Fine-tuning performance Curves of different methods across three seeds on MuJoCo expert datasets. The mean and standard deviation are shown by the solid lines and the shaded areas, respectively.